

THE EFFECT OF SPONTANEOUS POLARIZATION ON TWO-DIMENSIONAL ELASTICITY OF SMECTIC LIQUID CRYSTALS

P. V. Dolganov^{a}, V. K. Dolganov^{a,**}, P. Cluzeau^b*

^a*Institute of Solid State Physics, Russian Academy of Sciences
142432, Chernogolovka, Moscow Region, Russia*

^b*Université Bordeaux I, Centre de Recherche Paul Pascal, CNRS, Avenue A. Schweitzer
33600, Pessac, France*

Received January 14, 2013

The influence of polarity on orientational elasticity and on structures formed in the director field is studied in free-standing smectic films. Periodic stripe patterns and 2π -walls in a magnetic field are investigated. Measurements are performed on a nonpolar racemic mixture, on an optically pure ferroelectric compound, and in mixtures with different concentrations of the chiral isomers of opposite signs. The structure of periodic stripes changes drastically with the polarity of the film. The ratio of the bend K_B and splay K_S elastic constants for smectic films is determined as a function of polarization from the structure of periodic stripe patterns and 2π -walls. We find that the elastic anisotropy K_B/K_S increases essentially with increasing the polarity of the film. Changes of the elasticity and the structure of periodic stripes are explained by polarization charge effects.

DOI: 10.7868/S0044451013060219

1. INTRODUCTION

Oriental elasticity of ferroelectric liquid crystals [1] may differ essentially from elasticity of nonpolar materials. Splay of polarization gives rise to polarization charges [2], whose long-range self-interaction makes an additional contribution to the free energy. This electrostatic energy can be of the order of or even larger than the purely elastic energy and essentially influences the structure and elastic properties of ferroelectric liquid crystals. Nontrivial elasticity of polar liquid crystals has been investigated mostly using the light-scattering method [2–8] and via studies of line and point topological defects [8–15]. Renormalization of the elastic constants was found in light-scattering measurements of the Goldstone mode in ferroelectric liquid crystals [6, 7]. This result is supported by observations of different structure of point defects and spiral patterns in polar and nonpolar films [13–15]. But in spite of a long history of studies, the influence of polarization charges on elasticity is not completely understood.

Measurements of elastic properties in smectics are more difficult than in nematics due to the layer structure of the smectic phase and the dependence of the elasticity on polarity. Two-dimensional ($2D$) elasticity of the \mathbf{c} -director in smectics is described by the bend (K_B) and splay (K_S) elastic constants [2]. For a qualitative description of the elastic properties, the one-constant approximation $K_B = K_S$ is sometimes used. This approximation simplifies the analysis, but it is generally not justified by experiments in both polar and nonpolar smectics [2, 3, 8, 12, 15–17]: K_B may essentially differ from K_S and the elastic anisotropy K_B/K_S depends strongly on polarity. Renormalized by polarization charges, K_B is sometimes named the effective bend elastic constant. Investigations of the influence of polarity on elasticity are important both for fundamental physics and for potential applications of ferroelectrics. In particular, it has been demonstrated that polarization charges and the associated electric fields determine the orientation of molecules in liquid crystal cells and the electro-optic response [18].

Our investigations are performed with nonpolar and polar free-standing smectic films [19]. In the nonpolar Smectic- C ($\text{Sm}C$) phase, the long molecular axes are tilted with respect to the layer normal z by the polar

*E-mail: pauldol@issp.ac.ru

**E-mail: dolganov@issp.ac.ru

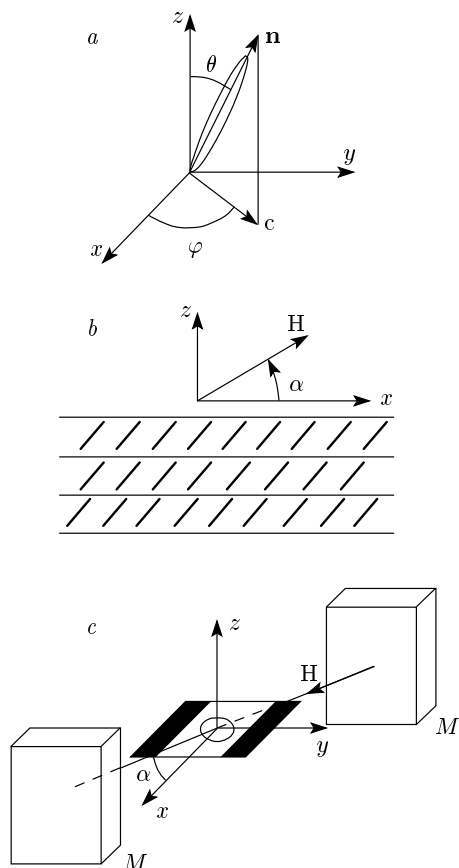


Fig. 1. Schematic representation of (a) SmC geometry, (b) a smectic film and (b,c) the geometry of measurements. \mathbf{n} is the average orientation of the long molecular axes, θ the tilt angle, \mathbf{c} the projection of \mathbf{n} onto the layer plane, and φ the azimuthal angle. The bars in (b) schematically show the liquid crystal molecules in smectic layers. Magnets (M) are located on two sides of the film. A magnetic field \mathbf{H} is applied in the xz plane at an angle α to the film plane (b,c)

angle θ (Fig. 1a). The films are formed by molecular layers parallel to the free surfaces (Fig. 1b). In the plane of the film, orientation of the molecules is described by the azimuthal angle φ or by the projection of the long molecular axes onto the xy plane, the so-called \mathbf{c} -director [1]. In the polar Smectic- C^* (SmC *) phase, the polarization vector \mathbf{P} lies in the smectic plane, locally normal to the \mathbf{c} -director.

To study the relation between elastic properties and polarization, Lee et al. [8] measured the elastic constants in mixtures of two SmC * compounds with different spontaneous polarization. To avoid effects of the molecular structure on elasticity, we performed studies using mixtures of two chiral enantiomers of the same

compound. We were able to vary the polarization of the medium by changing the enantiomer concentration and to directly study the dependence of the elasticity on polarization. Orientation elastic constants in polar and nonpolar films were determined from studies of periodic stripe structures and 2π -walls in a magnetic field. Periodic stripe structures differ drastically in nonpolar and polar films. Based of these observations, we found that the elastic anisotropy K_B/K_S increases with increasing polarization. In nonpolar films, the values of the bend K_B and splay K_S elastic constants are determined by the intermolecular interaction. In the polar isomer, the effective bend elastic constant K_B mostly depends on the electrostatic interaction of polarization charges. The polarization contribution to the ratio of elastic constants increases nonlinearly with the polarization. Our experimental results correlate with theory [8] describing the influence of polarization charges on elasticity.

2. EXPERIMENT

We performed the experiments on films composed of chiral *S*-4'-undecyloxybiphenyl-4-yl 4-(1-methylheptyloxy)benzoate (11BMSHOB), a racemic mixture of *R* and *S* enantiomers, and polar mixtures with different isomer concentrations. In the bulk sample, 11BMSHOB exhibits the following transition temperatures: SmC * -(108.3 °C)-N * -(123.9 °C)-I in the chiral material [20] and SmC-(108.3 °C)-N-(124 °C)-I in the racemic mixture. The polarization of the pure chiral material P_0 is about 120 esu/cm 2 and is practically independent of temperature. To prepare films with different polarizations, we used mixtures of the racemate and polar isomer. The polarization of the mixture is taken as $P = XP_0$ [6], with X defined as the fraction of the uncompensated polar isomer (excess of the polar isomer) in the mixture, which means that $X = 0$ in the racemate and $X = 1$ in the optically pure compound.

Free-standing films are prepared by spreading a tiny amount of the compound in the smectic phase over a 3-mm circular hole in a glass plate. Measurements are performed on films with a thickness of 8–10 smectic layers. An electric field is applied in the film plane using a pair of electrodes. The cell with the film could be inserted into a temperature-controlled oven between two permanent magnets (Fig. 1c). The direction of the magnetic field may be tilted with respect to the film plane (Fig. 1b,c). In most measurements, the magnetic field value was ~ 3 kOe, which is sufficient to orient the director in the nonpolar sample.

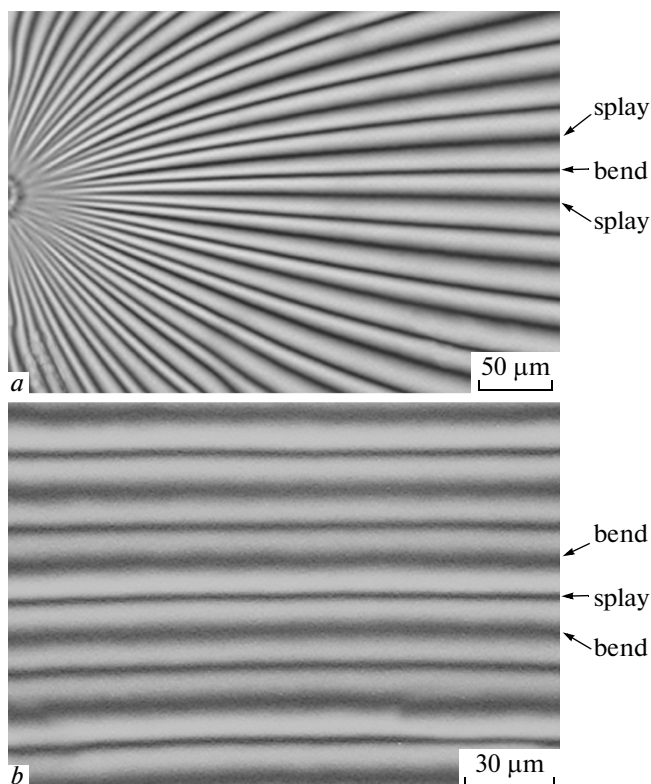


Fig. 2. (a) Structure with the radial stripe orientation that was formed due to the motion of the material from meniscus to the film center, $T = 103^\circ\text{C}$, racemic 11BSMHOB. (b) Periodic stripe structure in the optically pure isomer. The different width of the dark stripes is related to the elastic anisotropy ($K_S \neq K_B$). In the racemic mixture, regions with splay deformation are broader than regions with bend deformation, while in the chiral isomer, regions with bend deformation are broader than regions with splay deformation. The stripe appearance shows that $K_S > K_B$ in the racemate and $K_S < K_B$ in the pure chiral isomer. The polarizer and the analyzer are in the vertical and horizontal direction

After spreading, the film thickness is typically not uniform. Uniform thickness is achieved by keeping the film at a constant temperature for about half an hour. The resulting films are studied in polarized light (PL), using reflected light microscopy with crossed polarizers (RLMCP) and depolarized reflected light microscopy [21]. Using a combination of these methods, we were able to determine the azimuthal orientation of the \mathbf{c} -director in the films. The microscope images were captured by a CCD-camera.

Different methods have been used previously to prepare periodic stripe structures. They can be generated in smectic films mechanically [22], in a rotating [11, 14]

or AC [22, 23] electric field. In our experiments, we used two methods to obtain the stripe structure in films of 11BSMHOB. In nonpolar films, the periodic \mathbf{c} -director orientation can be prepared when additional smectic layers appear in the film. We observed formation of the stripe structure when the film was heated above the bulk transition temperature T_B and then cooled to below T_B . At low temperature, a part of the material moves from the meniscus towards the center of the film and may form a film of uniform thickness with a radial stripe structure (Fig. 2a). Since the number of stripes remains constant, the stripe period essentially decreases from the edge to the film center. The resulting stripe structure may exist in the film for a long time (more than an hour), which allows performing measurements.

In polar SmC^* films, periodic structures are obtained by applying an AC electric field to the film in a circular hole. In a certain range of field frequencies and values, periodic reorientation of the \mathbf{c} -director leads to the formation of an array of 2π -walls. In our experiments, the frequency of the field was 0.1–1 Hz, and its magnitude 0.02–0.033 statvolts/cm. After switching off the field, the structure of the 2π -walls relaxes. During relaxation, a stripe structure with a nearly constant period may form. The mechanism of the formation of the stripe structure was discussed in detail in Ref. [24]. Figure 2b shows a part of the polar film with a nearly parallel stripe texture. The stripe texture can remain in the film for several minutes. The number of stripes and their period depend on the value of the electric field and the duration of application. Most measurements were performed on stripe structures with the 25–50 μm periodicity.

Isolated 2π -walls were obtained in an external magnetic field. As a rule, in absence of the field, the \mathbf{c} -director in the film varies smoothly, not forming distinctive linear defects. After applying a magnetic field tilted with respect to the film plane, the director in most part of the film orients uniformly, except for relatively narrow regions in which 2π -walls are formed. If the ends of an isolated wall are pinned on the opposite edges of the sample, the wall cannot disappear. It is also possible to introduce a 2π -wall in the system by a 180° -reorientation of the \mathbf{c} -director. In nonpolar films, 2π -walls are formed by rotating the film with respect to the magnetic field direction such that the tilting angle α (Fig. 1b) changes its sign. This rotation induces a 180° -reorientation of the \mathbf{c} -director in the film plane, which can result in formation of 2π -walls [12, 16]. The 2π -walls in nonpolar films composed of a racemic mixture are investigated in a magnetic field. The structure

of the stripe pattern in films composed of heterochiral mixtures with different enantiomeric excess is studied without an external field.

3. EXPERIMENTAL RESULTS AND DISCUSSION

Periodic stripe structures

Periodic stripe structures are investigated in both nonpolar and polar films. To analyze the crossover from nonpolar films to pure chiral 11BMSHOB, we studied stripe structures in films composed of mixtures with different isomer concentrations.

Figure 2 shows RLMCP images of periodic stripes in a nonpolar SmC film prepared from the racemic mixture and in a SmC* film composed by the optically pure isomer. The **c**-director orientation was determined by combining RLMCP and PL. The dark stripes

in RLMCP correspond to **c**-director orientation parallel to one of the polarizers. In the center of the dark stripe, the deformation is pure bend or pure splay (the right side of Fig. 2). A schematic representation of the periodic stripe structure is given in Fig. 3a. The different widths of the dark stripes in Fig. 2 are related to the elastic anisotropy of the **c**-director field. The wider stripe corresponds to larger elastic constant. We found that narrow and wide black stripes in nonpolar and polar films correspond to different types of deformation. In nonpolar films, the regions with splay deformation are wider than those with bend deformation (Fig. 2a). This result indicates that $K_S > K_B$. On the contrary, in the pure chiral isomer, the regions with splay deformation are narrower than the regions with bend deformation (Fig. 2b), and hence $K_S < K_B$. For a quantitative description of the elasticity, the distances w_B and w_S between two bright stripes with bend and splay deformations in the middle are measured. The ratio w_B/w_S is used to determine the elastic anisotropy K_B/K_S in the films as a function of the enantiomer concentration.

The free energy of a smectic film in an external field can be written as [2]

$$F = h \int \left[\frac{1}{2} K_S (\nabla \cdot c)^2 + \frac{1}{2} K_B (\nabla \times c)^2 + F_{in} \right] dx dy, \quad (1)$$

where h is the film thickness. The **c**-director is a 2D unit vector with coordinates $(\cos \varphi, \sin \varphi)$. The first two terms in (1) are the two-dimensional elastic energy with splay and bend elasticity. In an external magnetic field, the last term (F_{in}) is the coupling between the field and the **c**-director orientation.

Minimizing (1) with respect to $\varphi(x, y)$ gives the equilibrium director configuration. For $K_S = K_B$ (which corresponds to the one-constant approximation), the Euler–Lagrange equation following from the minimum condition for (1) is simplified and its solution can be expressed in elementary functions for stripes and walls in magnetic and electric fields [9, 10, 16, 24]. But in general $K_S \neq K_B$, and an analytic expression for periodic stripe structures cannot be given. Therefore, to obtain the structures of periodic stripes ($F_{in} = 0$), the Euler–Lagrange equations should be solved numerically.

We consider the linear stripe structure parallel to the y axis. The Euler–Lagrange equation derived from (1) leads to the equation for the azimuthal orientation of the **c**-director $\varphi(x)$ across the stripes:

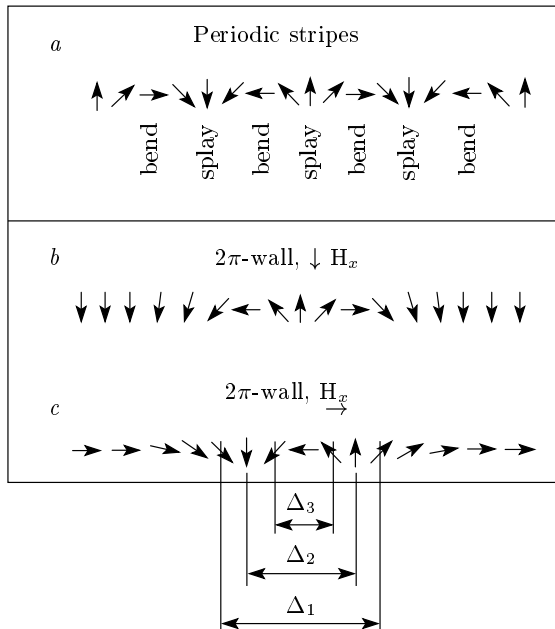


Fig. 3. Schematic representation of the **c**-director orientation across (a) a periodic stripe structure and (b, c) 2π -walls for different orientations of the walls with respect to the magnetic field. (b) The 2π -wall is oriented parallel to the **c**-director at a large distance from the wall. (c) The 2π -wall is oriented perpendicular to the **c**-director at a large distance from the wall. The main type of deformation in different regions of the periodic structure (bend or splay) is indicated in the lower part of (a). The widths Δ_1 , Δ_2 , and Δ_3 of the 2π -walls (the lower part of the figure) are measured to characterize the film elasticity

$$x - x_0 = A \int_{\varphi(x_0)}^{\varphi(x)} \sqrt{K_S \sin^2 \varphi + K_B \cos^2 \varphi} d\varphi, \quad (2)$$

where the constant A depends on the period of the structure. Periodic structures are the metastable states with respect to the uniformly oriented film.

Equation (2) allows determining the elastic anisotropy K_B/K_S from the experimental data. The distances between neighboring white stripes (Fig. 2) correspond to a rotation of φ by $\pi/2$. The relative width of w_B and w_S is a function of the ratio K_B/K_S and can be written as

$$\frac{w_B}{w_S} = \frac{\int_{3\pi/4}^{5\pi/4} \sqrt{\sin^2 \varphi + \frac{K_B}{K_S} \cos^2 \varphi} d\varphi}{\int_{\pi/4}^{3\pi/4} \sqrt{\sin^2 \varphi + \frac{K_B}{K_S} \cos^2 \varphi} d\varphi}. \quad (3)$$

The ratio w_B/w_S is calculated as a function of K_B/K_S . Comparing the experimentally measured ratio w_B/w_S with the results of the calculation, we determined the elastic anisotropy K_B/K_S . This procedure was performed for films composed of different mixtures. The results are given in Fig. 4 by circles as a function of the enantiomer concentration X and polarization P in the sample. We can see that K_B/K_S essentially increases with X and P .

2π-walls in a magnetic field

2π-walls are formed in a magnetic field tilted with respect to the film plane. Due to the positive diamagnetic anisotropy of the molecules, the minimum energy corresponds to the smallest possible angle between the long molecular axis and \mathbf{H} . Far from the 2π-wall, the \mathbf{c} -director is oriented parallel to the projection of \mathbf{H} on the film plane H_x (Fig. 3b,c).

Figure 5 shows photographs of 2π-walls with orientation perpendicular and parallel to H_x . In RLMCP with the polarizer parallel to H_x , 2π-walls appear as four bright stripes on a dark background (Fig. 5). These bright stripes correspond to the director orientation $\varphi = (2m + 1)\pi/4$, where m is an integer. A schematic representation of 2π-walls parallel and perpendicular to H_x is shown in Fig. 3. The inner structure of the walls gives information about the elastic constants. The \mathbf{c} -director orientation and deformation type in the same regions of two walls in Fig. 5 are different. In the middle of the central dark stripe (Fig. 5a), the director orientation is horizontal, which

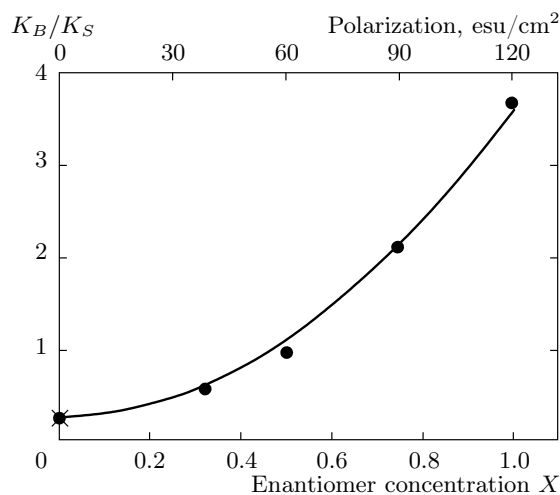


Fig. 4. Dependence of K_B/K_S on the enantiomer concentration X and polarization P . Circles are the data obtained from studies of periodic stripe structures. The cross shows the value of the elastic anisotropy in a non-polar film ($X = 0$) obtained from the structure of 2π -walls in a magnetic field. The solid line is a fit with a square function. Polarization (upper axis) was determined from the relation $P = XP_0$, where P_0 is the polarization in the pure chiral isomer ($X = 1$)

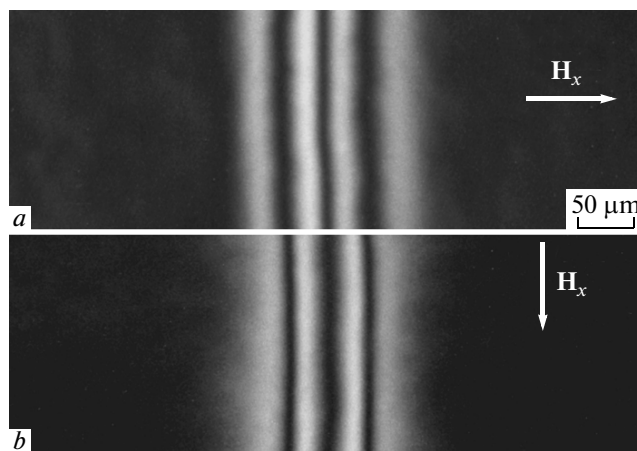


Fig. 5. 2π-walls in a magnetic field in a racemic 11BSMHOB film. (a) The wall is oriented perpendicular to the projection of \mathbf{H} on the film plane H_x . (b) The wall is oriented parallel to H_x . The photographs were taken in RLMCP, $T = 103^\circ\text{C}$, $H \approx 3 \text{ kOe}$, $\alpha = 16.9^\circ$

corresponds to bend deformation (Fig. 3c). In the middle of two broad dark stripes (Fig. 5a), the director is oriented vertically, and the deformation corresponds to splay (Fig. 3c). On the contrary, in the center of the

broad dark stripe in a 2π -wall parallel to \mathbf{H}_x (Fig. 5*b*), the \mathbf{c} -director orientation is vertical with splay deformation, and in two side stripes, the orientation is horizontal, which corresponds to a bend deformation. The halfwidth Δ_2 of a 2π -wall (Fig. 3), i. e., the distance between points where the \mathbf{c} -director is rotated by $-\pi/2$ and $+\pi/2$ with respect to the center, very slightly depends on the wall orientation, since the wall contains a combination of bend and splay between these points. By contrast, for $K_S \neq K_B$, the width Δ_3 (Fig. 3) between central bright stripes (Fig. 5) strongly depends on the wall orientation with respect to the field direction. The reason is that in the central part of the wall, the deformation of the \mathbf{c} -director is mainly of one type (bend or splay). Figure 5 clearly shows that the black stripes with splay deformation are broader than the ones with bend deformation. Hence, the structure of 2π -walls indicates that $K_S > K_B$ in the racemic mixture. To determine elastic anisotropy, the widths Δ_1 and Δ_3 (Figs. 3 and 5) between the points where the \mathbf{c} -director is rotated from $-3\pi/4$ to $+3\pi/4$ (Δ_1) and from $-\pi/4$ to $+\pi/4$ (Δ_3) were measured. A quantitative description of the elastic anisotropy is given later in this section.

The coupling between the field and the molecular orientation is given by $F_{in} = -1/2 \cdot \chi H^2 (A_1 \cos \varphi + A_2 \cos 2\varphi)$, where χ is the diamagnetic anisotropy, $A_1 = 1/2 \cdot \sin 2\theta \sin 2\alpha$, $A_2 = 1/2 \cdot \sin^2 \theta \cos^2 \alpha$, and α is the angle between the magnetic field and the film plane [16]. In F_{in} , we write only the terms dependent on φ . The structure of the wall can be obtained by numerical integration of the equation

$$\varphi' = \left[\frac{\chi H^2 (A_1 + A_2 - A_1 \cos \varphi - A_2 \cos 2\varphi)}{K_S K_\varphi} \right]^{1/2} \quad (4)$$

which follows from minimization of energy (1). In Eq. (4), $\varphi' = d\varphi/dx$ and $K_\varphi = \sin^2 \varphi + K_B/K_S \cos^2 \varphi$ for the wall perpendicular to H_x , $\varphi' = d\varphi/dy$ and $K_\varphi = \cos^2 \varphi + K_B/K_S \sin^2 \varphi$ for the wall parallel to H_x .

As mentioned above, the halfwidth of a 2π -wall Δ_2 very slightly depends on the wall orientation even for $K_S \neq K_B$. To determine K_B/K_S , two other regions Δ_1 and Δ_3 were used. In RLMCP observations, Δ_3 and Δ_1 are respectively the distances between two central and two outer bright stripes of the wall (Fig. 5). The regions Δ_3 and $(\Delta_1 - \Delta_3)$ correspond mainly to splay and bend distortions in 2π -walls parallel to H_x and conversely in 2π -walls perpendicular to the field (Fig. 3*b,c*). The ratio of these widths can be written as

$$\begin{aligned} \frac{\Delta_1 - \Delta_3}{\Delta_3} &= \\ &= \frac{2 \int_{\pi/4}^{3\pi/4} \left(\frac{K_\varphi}{A_1 + A_2 - A_1 \cos \varphi - A_2 \cos 2\varphi} \right)^{1/2} d\varphi}{\int_{3\pi/4}^{\pi/4} \left(\frac{K_\varphi}{A_1 + A_2 - A_1 \cos \varphi - A_2 \cos 2\varphi} \right)^{1/2} d\varphi}. \quad (5) \end{aligned}$$

This ratio, as well as w_B/w_S in Eq. (3), depends on K_B/K_S . To determine the elastic anisotropy, the ratio $(\Delta_1 - \Delta_3)/\Delta_3$ was calculated using (5) as a function of K_B/K_S . The elastic anisotropy was determined by fitting the experimental data by the calculated values. From the widths of 2π -walls, we obtain $K_B/K_S = 0.27$, which is close to the value obtained from measurements in periodic stripe structures (Fig. 4).

We now discuss the difference of K_B/K_S in non-polar and polar films. In a polar film with \mathbf{P} perpendicular to the \mathbf{c} -director, the bend-type deformation of \mathbf{c} leads to splay-type deformation of the polarization. This gives rise to polarization space charges with the density $\delta = -(\nabla \cdot \mathbf{P})$. Interaction of polarization charges with each other increases the energy of the film and effectively renormalizes the bend elastic constant. Without free charges, the change of K_B depends on the wavevector q of the deformation [2, 6, 13], and K_B should diverge as $q \rightarrow 0$. However free charges present in the film partially screen polarization-induced charges, and therefore the divergence is not achieved. The electrostatic energy depends on the ratio of $1/q$ and the $2D$ Debye screening length λ . As shown in [8] in the long-wavelength limit $q \ll 1/\lambda$, the effective elastic constant K_B is independent of q , and the part of the constant dependent on the polarization is proportional to P^2 . This dependence is valid if $1/q$ or the characteristic length on which the orientation of the \mathbf{c} -director changes sufficiently (i. e., the halfwidth Δ_2 in 2π -walls) is much larger than λ . The estimation for λ given in [8] is $\lambda \leq 1\mu\text{m}$. The period of stripe structures that correspond to the data in Fig. 4 was $25\text{--}50\mu\text{m}$, and the long-wavelength approximation should therefore be valid for our periodic stripe structures. Our experimental situation corresponds to the theoretical limit [8] where the wave vector dependence of the free energy does not play an important role.

The solid line in Fig. 4 for K_B/K_S shows the least-square fit of the data with squared functions $K_B/K_S = K_B^0/K_S + \beta P^2$, where K_B^0 is the bare bend elastic constant. The experimental results (Fig. 4) are in agreement with the theoretical predictions.

Previously, different configurations of point topological defects with the topological charge $S=+1$ were reported in polar and nonpolar films [13,26]. In polar films, the defects have a radial (splay) configuration of the \mathbf{c} -director, and in nonpolar or low-polarization films, they have a circular (bend) configuration. This finding was explained by an increase in effective bend elasticity in polar films and the energy of the circular configuration due to polarization charges [13,26]. In our case, as follows from Fig. 4, the critical concentration when the splay and bend elastic constants become equal is approximately 0.5. The transition from the circular to the radial director configuration observed in 11B5MHOB [26] is in agreement with our measurements.

The question exists about the origin of the difference between K_S and K_B in nonpolar films. The 2D smectic elastic constants are related to the bulk splay K_{11} , twist K_{22} , and bend K_{33} nematic elastic constants [2]. The elastic anisotropy in a nonpolar film may reflect the difference of the elastic constants in the nematic phase.

4. SUMMARY

In the investigations presented here, we study 2D elasticity in smectic films. The magnitude of the bare ratio K_B/K_S was determined in the racemic mixture from the structure of periodic stripes and 2π -walls in a magnetic field. Periodic stripe structures were used to study the influence of polarization on elasticity. The dependence of the elastic anisotropy K_B/K_S on polarization was determined in the static limit where the effective period of orientational deformation is much larger than the 2D Debye screening length λ . Our observations indicate that polarization charges induce a strong renormalization of the bend elastic constant. Polarization-dependent contributions to the elastic anisotropy and to the bend elastic constant show a P^2 behavior, in agreement with theoretical prediction [8]. The results of our investigation demonstrate the importance of the polarization space charges for the elastic properties of liquid crystals and are relevant for both fundamental physics and numerous technical applications.

This work was supported in part by the RFBR projects 12-02-33124, 11-02-01028, and 11-02-01424. We thank H. T. Nguyen, A. Babeau, and S. Gineste for synthesis of the liquid crystals.

REFERENCES

1. P. G. de Gennes and J. Prost, *The Physics of Liquid Crystals*, 2nd ed., Clarendon Press, Oxford (1993).
2. C. Y. Young, R. Pindak, N. A. Clark, and R. B. Meyer, *Phys. Rev. Lett.* **40**, 773 (1978).
3. C. Rosenblatt, R. Pindak, N. A. Clark, and R. B. Meyer, *Phys. Rev. Lett.* **42**, 1220 (1979).
4. D. H. Van Winkle and N. A. Clark, *Phys. Rev. A* **38**, 1573 (1988).
5. S. M. Amador and P. S. Pershan, *Phys. Rev. A* **41**, 4326 (1990).
6. M.-H. Lu, K. A. Crandall, and C. Rosenblatt, *Phys. Rev. Lett.* **68**, 3575 (1992).
7. Y. Galerne, I. Poinot, and D. Schaegeis, *Appl. Phys. Lett.* **71**, 222 (1997).
8. J. B. Lee, R. A. Pelcovits, and R. B. Meyer, *Phys. Rev. E* **75**, 051701 (2007).
9. R. Pindak, C. Y. Young, R. B. Meyer, and N. A. Clark, *Phys. Rev. Lett.* **45**, 1193 (1980).
10. D. R. Link, L. Radzihovsky, G. Natale et al., *Phys. Rev. Lett.* **84**, 5772 (2000).
11. Y. Galerne and R. Najjar, *Phys. Rev. E* **69**, 031706 (2004).
12. P. V. Dolganov, B. M. Bolotin, and A. Fukuda, *Phys. Rev. E* **70**, 041708 (2004).
13. D. R. Link, N. Chattham, J. E. Maclennan, and N. A. Clark, *Phys. Rev. E* **71**, 021704 (2005).
14. A. Eremin, C. Bohley, and R. Stannarius, *Eur. Phys. J. E* **21**, 57 (2006).
15. A. Eremin, C. Bohley, and R. Stannarius, *Phys. Rev. E* **74**, 040701(R) (2006).
16. P. V. Dolganov and B. M. Bolotin, *Pis'ma Zh. Eksp. Teor. Fiz.* **77**, 503 (2003) [*JETP Lett.* **77**, 429 (2003)].
17. P. V. Dolganov, V. K. Dolganov, and P. Cluzeau, *Pis'ma Zh. Eksp. Teor. Fiz.* **96**, 347 (2012) [*JETP Lett.* **96**, 317 (2012)].
18. D. Coleman, D. Muller, N. A. Clark et al., *Phys. Rev. Lett.* **91**, 175505 (2003).

19. P. Pieranski, L. Bieliard, J.-Ph. Tournelles et al., *Physica A* **194**, 364 (1993).
20. P. Cluzeau, M. Ismaili, A. Annakar et al., *Mol. Cryst. Liq. Cryst.* **362**, 185 (2001).
21. D. R. Link, G. Natale, R. Shao et al., *Science* **278**, 1924 (1997).
22. P. E. Cladis, Y. Couder, and H. R. Brand, *Phys. Rev. Lett.* **55**, 2945 (1985).
23. S. Uto, E. Tazoh, M. Ozaki, and K. Yoshino, *Jpn. J. Appl. Phys.* **36**, L1198 (1997).
24. R. Najjar and Y. Galerne, *Mol. Cryst. Liq. Cryst.* **366**, 421 (2001).
25. R. Stannarius, J. Li, and W. Weissflog, *Phys. Rev. Lett.* **90**, 025502 (2003).
26. P. V. Dolganov, H. T. Nguyen, G. Joly, V. K. Dolganov, and P. Cluzeau, *Europhys. Lett.* **76**, 250 (2006).